PHYSICAL REVIEW B VOLUME 27, NUMBER 4 15 FEBRUARY 1983

Distribution of activation energies for impurity hopping in amorphous metals

Peter M. Richards
Sandia National Laboratories, Albuquerque, New Mexico 87185
(Received 17 September 1982)

The distribution of activation energies Δ for classical over-the-barrier hopping is computed for a model amorphous metal. The spread in Δ is determined by the variation in equilibrium-site and saddle-point sizes for the assumed model of dense random packing (DRP) of soft spheres. The size distribution is related to the radial distribution function in a manner which reproduces recent numerical results for the interstitials in DRP models. Size (distance) variation in general is related to energy variation by the form of the potential energy $V(r)$. We show, however, that the distribution of equilibrium-site energies can be related directly to the impurity-induced lattice expansion and bulk modulus without detailed knowledge of $V(r)$. The form of $V(r)$ is necessary for the saddle-point distribution, and we estimate this using simple analytic expressions which fit the observed lattice expansion and impurity (hydrogen) vibrational frequency. The effects of a hard core plus lattice relaxation at the saddle point are also considered. Specific account is taken of the correlation between saddle-point and equilibrium-site configurations in the computation of the distribution of Δ. Results are compared with recent data on hydrogen internal friction in amorphous $Pd_{80}Si_{20}$ and good agreement is found between our *first-principles* distribution and that used to fit the data.

I. INTRODUCTION

The structure of amorphous metal and metal-metalloid alloys has been of interest to many workers[1] for some time. More recently, bulk diffusion and internal friction of small amounts of hydrogen have been studied in these systems.[2,3] Internal friction[4] is a measure of local hopping among different sites. For a random system it is reasonable that such hopping be characterized by a distribution of activation energies since the sites have nonuniform environments. Indeed the internal friction for H in $Pd_{80}Si_{20}$ shows a non-purely-Debye character which was fit to a rather broad distribution of activation energies.[3]

Non-Debye relaxation [i.e., lack of single relaxation (correlation) time which has an Arrhenius temperature dependence] is well known to be observed—more often than not[5]—in experiments on dielectric relaxation and NMR as well as on internal friction. The data are frequently, as in Ref. 3, described by a distribution of relaxation times with varying activation energies. However, I am aware of no previous work in which the width of the distribution has been calculated *a priori*, although an estimate for the distribution of *site* energies has been given.[6] Thus the description is largely phenomenological, and a major question remains: Is the required spread of activation energies plausible in terms of the structure and interactions? This paper addresses just that question and answers in the affirmative for the data on H in $Pd_{80}Si_{20}$.

The question assumes additional importance in light of the proposed[5] "universal response function." In that model a time correlation function of the form $\exp[-(t/\tau)^p]$ is assumed with $0<p\leq 1$ ($p=1$ is the usual Debye case with a single correlation time τ). It is argued that such a function, which works very well as long as p is chosen to fit the data, has more fundamental significance than a distribution of relaxation times. The need for such an additional "intrinsic" non-Debye relaxation should hinge to some extent on whether it is reasonable to expect distributions of the required widths.

The distribution of activation energies for a particle hopping in an amorphous metal is governed by (i) the distribution of particle—metal-ion distances at interstitial holes and saddle points and (ii) the particle—metal-ion potential as a function of distance. We assume that the diffusion is classical hopping between equilibrium interstitial positions which are separated by a saddle-point barrier. Thus the activation energy is simply the difference between saddle-point and local-minimum potentials (with proper account taken for the zero-point vibrational energy at the minimum). Any tunneling, phonon assisted or otherwise, is neglected. This classical picture is thought to be acceptable for H dif-

fusion[7] in fcc Pd, though it clearly is not for the bcc metals.

Assuming classical hopping, one must therefore delineate the interstitial holes and saddle points for a random system. This has largely been done for models of the dense random packing (DRP) of spheres.[8,9] The salient feature for the present work is that the sites are predominantly at the centers of tetrahedra and octahedra, which are in general distorted from their regular shapes in a crystal. The faces of these polyhedra form triangles, the centers of which may be taken as saddle points. Ahmadzadeh and Cantor[9] have further provided distributions for the sizes of the octahedra, tetrahedra, and triangles. From these, together with a suitable hydrogen-metal potential, a distribution of activation energies can be constructed. In fact, they pointed this out themselves,[9] although they were content with calculating only an average activation energy by a questionable (see Sec. IV) procedure. I show here that the relevant quantity for determining the site (saddle-point) energy is the sum of the lengths of the polyhedron edges (sides of the triangle) and that the distribution for such can be related simply to the pair radial distribution function (RDF). In this manner one can actually predict some of the interstitial-size distributions found in Ref. 9.

The hydrogen-metal potential is difficult to obtain from first principles. As in Ref. 6, it is shown that the width of the equilibrium-site energy distribution is directly related to the hydrogen-induced lattice expansion. Thus one actually does not need to construct a model potential in this case. Consideration of the saddle-point energy distribution, however, is more tenuous, and it is discussed in terms of simple analytic potentials with parameters chosen to fit the observed lattice expansion and hydrogen vibrational frequency in crystalline Pd. Effects of a hard-core and lattice relaxation are also treated.

Section II presents a general theory for computing the distribution of activation energies in terms of the RDF, assuming the potential is known. Application to H in $Pd_{80}Si_{20}$ is made in Sec. III, where questions such as modeling the potential and which type of site (octahedral or tetrahedral) is occupied are addressed. Discussion of several points is made in Sec. IV, and the paper is summarized in Sec. V.

II. THEORY

In this section we express the energy of a particle at equilibrium inside a geometrical figure in terms of the dimensions of the figure and then show how to express the resulting energy distribution in terms of the RDF. Consider a regular figure of n vertices centered at the origin. The displacement from the origin to the ith vertex is $\vec{R}_i^0$ with each $\vec{R}_i^0$ having the same magnitude R_0. Figure 1 illustrates the case for a triangle. A metal ion is at each vertex and a hydrogen at the center. If the hydrogen-metal potential $V(\vec{R})$ is central [$V(\vec{R})=V(R)$], it is evident that the origin is a position of equilibrium, though not necessarily stable, as long as

$$\sum_{i=1}^{n} \vec{R}_i^0 = 0 , \tag{1}$$

and the energy is $U_0=nV(R_0)$, assuming nearest-neighbor interactions only. Now let the positions of the vertices be changed to $\vec{R}_i=\vec{R}_i^0+\vec{r}_i$. We show in Appendix A that the new *equilibrium* energy is, to lowest order in $\vec{r}_i$,

$$U=U_0+\frac{n}{N}\sum_{i=1}^{N}(d_i-d_0)\left[\frac{R_0}{d_0}\right]V'(R_0) , \tag{2}$$

where N is the number of edges of the figure, d_0 is the edge length of the regular figure, and d_i is the length of the ith edge of the distorted figure. Table I lists the values of n, N, and R_0/d_0 for the figures of interest: triangle, tetrahedron, and octahedron. As is common practice, we work in units of d_0, which is the hard-sphere diameter, assuming the figures correspond to close-packed arrangements of spheres. In the study of elastic effects of hydrogen[10] and other defects, it is convenient to define a dipole force tensor

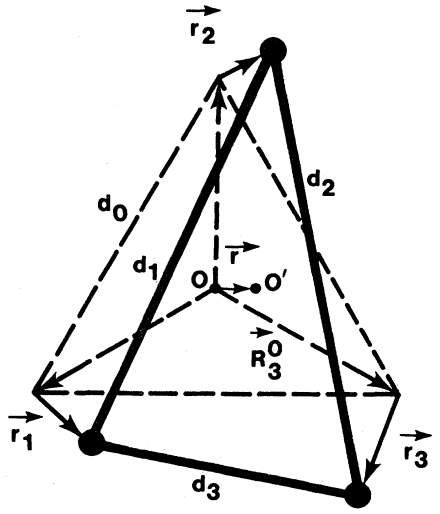

FIG. 1. Host atoms forming distorted triangle of sides d_1, d_2, and d_3 made by displacing ith vertex of equilateral triangle (side d_0) by $\vec{r}_i$. The equilibrium position for impurity shifts by $\vec{r}_i$ from 0 to 0'.

TABLE I. Some useful geometry for regular figures. n is the number of edges of length d_0, N is the number of vertices, and R_0 is the distance from center to vertex.

Figure	n	N	R_0/d_0
Triangle	3	3	$1/\sqrt{3}$
Tetrahedron	4	6	$\sqrt{3/8}$
Octahedron	6	12	$1/\sqrt{2}$

$$P_{\alpha\beta}=\sum_{i=1}^{n} F_{i\alpha}R_{i\beta}^{0}\ , \tag{3}$$

where $F_{i\alpha}=-\partial V/\partial R_{i\alpha}$ is the α ($\alpha=x$, y, or z) component of the force exerted by the hydrogen on the metal ion originally at $\vec{R}_{i,0}$ and $R_{i\beta}^{0}$ is the corresponding β component of $\vec{R}_i$. Since

$$F_{i\alpha}=-(R_{i\alpha}^{0}/R_0)V'(R_0)\ ,$$

we have

$$\mathrm{Tr}P_{\alpha\beta}\equiv 3P=-nR_0V'(R_0)\ , \tag{3a}$$

so that Eq. (2) becomes

$$U=U_0-3P\left[(1/N)\sum_{i=1}^{N}\left[\frac{d_i}{d_0}-1\right]\right]\ , \tag{4}$$

in which P is the same as defined in Ref. 10 and the quantity in square brackets represents the mean percentage change in length of the edges from the regular figure. One can show further from the theory of elasticity[10,11] that

$$P=K\,\Delta V\ , \tag{5}$$

where K is the bulk modulus and ΔV is the change in sample volume per hydrogen atom. Equation (4) does not include a change in energy, proportional to P^2, brought about by relaxation of the metal lattice upon introduction of the hydrogen. However, as noted in Appendix A, this term is independent of $\vec{r}_i$ to lowest order, and so the above represents the complete first-order change in energy related to a distortion of the interstitial or saddle-point cage in going from the regular crystalline structure to the random one. A similar result is contained in Ref. 6.

According to Eqs. (4) and (5) the distribution of site energies is related to the distribution of *total* edge lengths with a proportionality which depends only on the bulk modulus and volume change. The distribution of any *one* edge length is the same as the nearest-neighbor RDF since the distance between adjacent vertices is just the neighboring metal-metal distance. If the lengths which make up the figure are uncorrelated, the total-length distribution is readily obtained from the RDF as

$$\rho_N(Y)=\int dy_1\cdots\int dy_N\rho(y_1)\cdots\rho(y_N)\times\delta\left[\sum_{i=i}^{N}y_i-Y\right]\ , \tag{6}$$

where $y_i\equiv d_i/d_0-1$, $\rho(y_i)$ is the RDF, and $\rho_N(Y)$ is the distribution for $\sum_{i=1}^{N}y_i=Y$. For a Gaussian RDF

$$\rho(y_i)=\exp(-y_i^2/\sigma^2)\ , \tag{7}$$

in which σ is the halfwidth at $1/e$ height of the RDF in units of the hard-sphere diameter d_0, we have

$$\rho_N(Y)=\exp(-Y^2/N\sigma^2)\ . \tag{8}$$

as is evident from considering the problem as a random walk of N steps so that $\langle Y^2\rangle=N\langle y_i^2\rangle$. In Eqs. (7) and (8) and subsequent equations we ignore normalization constants in the distributions. For convenience the various lengths are illustrated and defined in Fig. 2 and the accompanying caption. Equation (8) contains a specific prediction about the distribution of interstitial sizes, which may be compared with results in Ref. 9. As in Appendix A, the average distance from the center of the figures to a vertex is $R_0+r=R_0+YR_0/Nd_0$; so the deviation r has a width given by $\sigma_r=\sigma R_0/N^{1/2}d_0$ according to Eq. (8). For the triangle and tetrahedron, we have $\sigma_r(\text{triangle})=\sigma/3$, $\sigma_r(\text{tetrahedron})=\sigma/4$. These appear to agree very well with the soft-sphere (relaxed) distributions shown in Figs. 3(b), 12(b), and 13(b) of Ref. 9. It follows from Eqs. (4), (5), and (8) that the $1/e$ width of the site energy distribution is

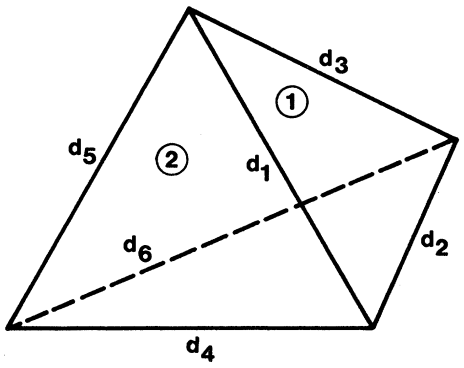

FIG. 2. Sample figure to illustrate notation. Here, for tetrahedron, number of faces $F=4$. $y_i=(d_i-d_0)/d_0$, d_0 is the edge length of regular figure. Face number 1, $Y_1=y_1+y_2+y_3=(d_1+d_2+d_3-3d_0)/d_0$; 2, $Y_2=y_1+y_4+y_5$; 3, $Y_3=y_3+y_5+y_6$; 4, $Y_4=y_2+y_4+y_6$. Total edge variation $Y=\sum_{i=1}^{6}y_i=\frac{1}{2}\sum_{\alpha=1}^{4}Y_\alpha$.

$$\delta U = 3K\,\Delta V\,\sigma N^{-1/2} \tag{9}$$

(K is the bulk modulus; ΔV, the volume change per hydrogen atom; σ, the RDF width in units of the hard-sphere diameter; N, the number of edges of the figure in which hydrogen is centered). This differs from the expression in Ref. 6 mainly in that it contains a factor N which relates specifically to the geometry of the site.

The distribution of activation energies is obtained in a similar manner with the following considerations. The net hopping rate out of equilibrium site i is defined as

$$W_i = \sum_\alpha w_{i\alpha} , \tag{10}$$

where $w_{i\alpha}$ is the rate to hop out of site i through the αth face of the polyhedron centered at site i. An important point in considering the distribution is that W_i—rather than the individual $w_{i\alpha}$—gives the observed hopping rate since the processes act in parallel.

It will be seen that the distribution of activation energies for the individual $w_{i\alpha}$ is much broader than that of W_i; so it is important that this distinction be made. The individual classical hopping rate $w_{i\alpha}$ at temperature T is

$$w_{i\alpha} = \nu_0 \exp(-\beta\Delta_{i\alpha}) , \tag{11}$$

where $\beta = 1/k_B T$, the prefactor ("attempt frequency") ν_0 is assumed to be uniform, as justified in Sec. IV, and the activation energy $\Delta_{i\alpha}$ is expressed as

$$\Delta_{i\alpha} = U_\alpha - U_i - \tfrac{3}{2}\hbar\omega_0 = \Delta_0 - a_s Y_\alpha + a_E Y_i , \tag{12}$$

where

$$Y_i = \sum_{k=1}^{N_E} y_k^{(i)} = \sum_{k=1}^{N_E} \left[\frac{d_k^{(i)}}{d_0} - 1 \right] , \tag{13}$$

in which $d_k^{(i)}$ is the length of the kth edge of the polyhedron centered at site i, and

$$a_E = -(n_E/N_E)V'(R_{0E})R_{0E} = 3\,\Delta V_E K/N_E . \tag{14}$$

E stands for equilibrium site; n_E and N_E are the number of vertices and edges, respectively, of the polyhedron (Table I). Similarly, s stands for the saddle point and

$$Y_\alpha = \sum_{k=1}^{N_s} y_k^{(\alpha)} = \sum_{k=1}^{N_s} \left[\frac{d_k^{(\alpha)}}{d_0} - 1 \right] , \tag{15}$$

$$a_s = -(n_s/N_s)V'(R_{0s})R_{0s} , \tag{16}$$

with n_s and N_s the saddle-point (face) quantities. ($N_s = n_s = 3$ for the triangular faces considered here.)

The activation energy Δ_0 is that for the ideal geometry of close-packed spheres. The zero-point energy $\frac{3}{2}\hbar\omega_0$ ($\omega_0/2\pi$ is the hydrogen vibrational frequency) has been included in (12) and is assumed to be the same at each site. We show in Sec. IV that the expected variation in ω_0 is small compared with the calculated width of the distribution of activation energies, so it is legitimate to treat ω_0 as constant.

The activation energy for hopping out of site i is defined as

$$\Delta_i = \partial \ln W_i/\partial\beta = \Delta_0 + a_E Y_i - a_s \frac{\sum_\alpha Y_\alpha e^{\beta a_s Y_\alpha}}{\sum_\alpha e^{\beta a_s Y_\alpha}} , \tag{17}$$

where the second equality is obtained from Eqs. (10)–(12). The summation over the faces in Eq. (17) makes Δ_i, in general, temperature dependent. But it is temperature independent in the limit of both low and high temperature. For sufficiently high temperature in which $|\beta a_s Y_\alpha| \ll 1$ the exponentials are replaced by unity and

$$\Delta(\text{high temperature}) = \Delta_0 + a_E Y - a_s \sum_{\alpha=1}^{F} Y_\alpha/F , \tag{18}$$

where F is the number of faces of the polyhedron. The subscript i has been and will continue to be dropped, it being understood that expressions refer to the ith site. At low temperatures summation is dominated by the largest Y_α (assuming $a_s > 0$) so that

$$\Delta_i(\text{low temperature}) = \Delta_0 + a_E Y_i - a_s Y_{\alpha\max} , \tag{19}$$

where $Y_{\alpha\max}$ is the maximum value for the figure. That is, one takes the face which has the largest perimeter and $Y_{\alpha\max}$ is the value of the deviation for this face as given by Eq. (15). Note that the low-temperature limit used here is still considered to be sufficiently high for classical hopping to apply.

The saddle-point quantities (coefficients of a_s) in Eqs. (18) and (19) are not at all independent of the total edge deviation Y. Indeed, the high-temperature expression $\sum Y_\alpha$ must be proportional to Y since both involve a sum over all the edges. For figures such as the tetrahedron and octahedron in which each edge is common to two faces, one has

$$\sum_{\alpha=1}^{F} Y_\alpha = 2 \sum_{k=1}^{N_E} \left[\frac{d_k}{d_0} - 1 \right] = 2Y , \tag{20}$$

so that Eq. (18) becomes

$$\Delta(\text{high temperature})=\Delta_0+\left[a_E-\frac{2a_s}{F}\right]Y . \tag{21}$$

In the present notation Eq. (2) for the site energy can be written as

$$U=U_0-a_E Y , \tag{22}$$

and so the high-temperature distribution of activation energies scales exactly with that of the site energies, but it can be considerably narrower if $|a_E-2a_s/F| \ll |a_E|$. It follows at once that

$$\delta\Delta(\text{high temperature}) = |1-2a_s/Fa_E|\,\delta U \tag{23}$$

where $\delta\Delta$ is the width of a Gaussian distribution of activation energies and δU is the corresponding width of the site energy distribution given by Eq. (9).

Contrary to one's first intuition, the low-temperature limit gives a broader distribution since $Y_{\alpha\max}$ in Eq. (19) is not uniquely determined by Y_i. In this case the distribution is

$$\rho(\Delta)=\int dY \int dY_{\alpha\max}\rho_{N_E}(Y)\rho(Y_{\alpha\max}\mid Y) \times\delta(\Delta-\Delta_0-a_E Y+a_s Y_{\alpha\max}) , \tag{24}$$

where $\rho_{N_E}(Y)=\exp(-Y^2/N_E\sigma^2)$ is the distribution for Y_i as in Eq. (8) and $\rho(Y_{\alpha\max}\mid Y)$ is the probability distribution of $Y_{\alpha\max}$ given Y. The calculation of $\rho(Y_{\alpha\max}\mid Y)$ is given in Appendix B.

For an octahedron it is

$$\rho(Y_{\alpha\max}\mid Y)=e^{-t^2}[\operatorname{erfc}(-t)]^7 , \tag{25}$$

where $t=2(Y_{\alpha\max}-Y/4)3\sigma$. The distribution $\rho(\Delta)$ can then be computed by using (25) in (24), but the form of $\rho(Y_{\alpha\max}\mid Y)$ precludes an analytic expression. Thus for general expressions we consider only the first and second moments

$$\langle\Delta\rangle_{\text{low temp}}=\Delta_0+(a_E-2a_s/F)\langle Y\rangle-a_s\langle\delta Y_{\alpha\max}\rangle , \tag{26}$$

$$\langle(\Delta-\langle\Delta\rangle)^2\rangle_{\text{low temp}}=(a_E-2a_s/F)^2\langle(Y-\langle Y\rangle)^2\rangle+a_s^2\langle(\delta Y_{\alpha\max}-\langle\delta Y_{\alpha\max}\rangle)^2\rangle \equiv\tfrac{1}{2}[\delta\Delta(\text{low temperature})]^2 , \tag{27}$$

where $\delta Y_{\alpha\max}=Y_{\alpha\max}-2Y/F$ is the departure of $Y_{\alpha\max}$ from the expectation value of any of the Y_α in the conditional distribution, and $\langle\delta Y_{\alpha\max}\rangle\neq 0$ since $Y_{\alpha\max}$ is defined as the largest of all the Y_α. The first term on the right-hand side of Eq. (27) is the corresponding expression in the high-temperature approximation Eq. (18). The second equality in (27) relates the second moment to the $1/e$ width of a Gaussian forced to fit the distribution with the same first and second moments. A correlation term proportional to $\langle Y\delta Y_{\max}\rangle - \langle Y\rangle\langle\delta Y_{\max}\rangle$ has been neglected in Eq. (27) because we show in Appendix B that it is zero for a Gaussian RDF.

An important question regards the effect of site occupation probability on the activation energy. If, for example, the Gaussian Eq. (8) were used to compute $\langle Y\rangle$, and thereby $\langle Y\rangle=0$ in Eqs. (26) and (27), it would be equivalent to paying no attention to the thermal probability for finding the particle at a given site. At least for situations in which relaxation is achieved in one jump, such a probability must be included. Hence the site distribution should be replaced by

$$\rho(Y_i)\rightarrow P_0(U(Y))\exp(-Y^2/N_E\sigma^2) , \tag{28}$$

where P_0 is the thermal equilibrium probability of finding the particle at site i and U is a function of Y via Eqs. (4) or (14). If only 1 particle per site is allowed, P_0 is the Fermi distribution

$$P_0=\{\exp[-\beta a_E(Y-Y_F)]+1\}^{-1} , \tag{29}$$

where Y_F is fixed by the hydrogen concentration. At low temperature Eq. (29) is replaced by $P_0=\Theta(Y-Y_F)$, where $\Theta(x)$ is the unit step function and Y_F is given by

$$c=\int_{-\infty}^{\infty} dY\,\Theta(Y-Y_F)\frac{\exp(-Y^2/N_E\sigma^2)}{\int_{-\infty}^{\infty} dY\exp(-Y^2/N_E\sigma^2)} =\tfrac{1}{2}\operatorname{erfc}(Y_F/N_E^{1/2}\sigma) , \tag{30}$$

where the effective concentration c is the number of hydrogen atoms per number of interstitial sites. This is equivalent to the expression found in Ref. 6. Validity of the zero-temperature approximation requires that, for a given Y_F, the same answer is obtained when the complete expression (29) is used instead of $\Theta(Y-Y_F)$ in the integrand of Eq. (30). We estimate that this requires

$$\exp(-\beta a_E N_E^{1/2}\sigma) \ll 1$$

and

$$\exp[-(\beta a_E N_E^{1/2}\sigma - 4Y_F/N_E^{1/2}\sigma)] \ll 1 .$$

For H in $Pd_{80}Si_{20}$ (Sec. III), $\beta a_E N_E^{1/2}\sigma \approx 9$ at 250 K and

$$\exp[-(9-4Y_F/N_E^{1/2}\sigma)] < 0.1$$

for $c \geq 1\%$ [using the second equality in Eq. (30)]. Thus replacement of (29) by the step function is justified except at extremely low hydrogen concentration and will be used henceforth. Thereby

$$\langle Y\rangle/N_E^{1/2}\sigma = z_0 f , \tag{31}$$

$$\langle (Y-\langle Y\rangle)^2\rangle/N_E\sigma^2 = \tfrac{1}{2}[1-2z_0^2 f(f-1)] , \tag{32}$$

where $z_0 = Y_F/N_E^{1/2}\sigma$ is given in terms of c by Eq. (31) and

$$f = e^{-z_0^2}/\sqrt{\pi z_0}\,\mathrm{erfc}(z_0)$$

($f \to 1$ for $z_0 \to \infty$). At $c = 0.01$, the values are $\langle Y\rangle/N_E^{1/2}\sigma = 1.88$ and

$$\langle (Y-\langle Y\rangle)^2\rangle/N_E\sigma^2 = 0.048 ,$$

the latter showing an extreme reduction in the second moment from its value without weighting with respect to the thermal equilibrium probability.

For completeness, we also consider the distribution $\rho(\Delta_{i\alpha})$ for jumping through a particular face α. This is obtained by replacing $\delta Y_{\alpha\max}$ with δY_α in Eqs. (26) and (27), and using the distribution $\rho(Y_\alpha \mid Y)$ given in Appendix B, for which $\langle \delta Y_\alpha\rangle = 0$. Since $\langle (\delta Y_\alpha^2)\rangle$ is about 2.5 times greater than $\langle (\delta Y_{\alpha\max} - \langle \delta Y_{\alpha\max}\rangle)^2\rangle$ (see Table III, Appendix B), this gives a much broader distribution of activation energies.

III. APPLICATION TO $Pd_{80}Si_{20}$

A basic premise in computing the energy distribution for hydrogen in the metal-metalloid glass $Pd_{80}Si_{20}$ is that the matrix can be treated as though it were a fictitious pure amorphous Pd. This may not be totally unreasonable since it is thought[12] that in such a binary glass the smaller Si atoms occupy the larger Bernal holes in the Pd structure. In this case the hydrogen would likely reside in the octahedral or tetrahedral sites completely surrounded by Pd atoms. It is further assumed that the potential for hydrogen in amorphous Pd is the same as in the crystalline material. Since hydrogen occupies the octahedral sites[13] in fcc Pd, it is natural to assume this for the amorphous material as well, at least at sufficiently low concentrations to be accommodated in the small (relative to the number in fcc) number of octahedral holes. The fact that the volume change per hydrogen[6,14] is nearly the same in crystalline Pd as in amorphous $Pd_{80}Si_{20}$ certainly is consistent with the concept of the same potential and same-type site occupation in the two systems. [See under Eq. (38) below, however.]

The bulk modulus of Pd is[15] $K = 1.8\times10^{12}$ erg/cm^3 $= 1.1$ eV/Å^3, and the volume change per hydrogen is[14] $\Delta V = 2.9$ Å^3. Thus Eq. (14) gives for the equilibrium-site parameter $a_E = 0.8$ eV with $N_E = 12$ for an octahedron. The RDF (Refs. 6 and 16) in $Pd_{80}Si_{20}$ has a full width at $1/e$ height of about 0.39 Å and is peaked at 2.75 Å; so in units of the sphere diameter, $\sigma = 0.07$, which agrees well with that given for the relaxed random-packing models.[8,9,17] The octahedral site energy width of Eq. (9) is then

$$\delta U = 0.19 \text{ eV} = 18 , \tag{33}$$

in kJ/mole, which is close to the value of 15 kJ/mole derived in Ref. 6 in a somewhat more phenomenological manner.

The saddle-point parameter a_s is required in addition to a_E for obtaining the width of the activation energy distribution. This could be obtained directly if the volume expansion for hydrogen at the saddle point was known. Since it is not known, we determine a_s from a model potential constructed to give the observed volume expansion and hydrogen vibrational frequency at the octahedral site. The volume expansion is related to the potential gradient via Eqs. (3a) and (5). The vibrational frequency ω_0 is related by

$$m\omega_0^2 = 2[V''(R_0) + 2V'(R_0)/R_0] , \tag{34}$$

where m is the mass of the hydrogen atom placed at the center of a regular octahedron of six metal ions each a distance R_0 away. Neutron data[18] show that $\hbar\omega_0 = 66$ meV for dilute H in crystalline Pd. This number converts to $m\omega_0^2 d_0^2 = 8.8$ eV for the sphere diameter $d_0 = 2.75$ Å. Equation (34) may be combined with Eqs. (3a) and (5) to give

$$\frac{R_0 V''(R_0)}{|V'(R_0)|} = \frac{m\omega_0^2 R_0^2}{K\Delta V} + 2 = 3.38 , \tag{35}$$

where $V'(R_0) < 0$ has been assumed and the final equality comes from taking the above numbers for $m\omega_0^2 R_0^2$, K, and ΔV ($R_0 = d_0/\sqrt{2}$). The quantities a_s and a_E are in the ratio

$$\frac{a_s}{a_E} = 2\left[\frac{2}{3}\right]^{1/2}\frac{V'(R_s)}{V'(R_0)} \tag{36}$$

according to Eqs. (14) and (16) ($R_s/R_0 = \sqrt{2/3}$,

TABLE II. Use of various functional forms for potential $V(R)=V(R_0)+Af(R)$. Parameters are chosen to fit observed lattice expansion and hydrogen vibrational frequency, as discussed in text. $\Delta V_T/\Delta V_0$ is the lattice expansion for hydrogen at the tetrahedral site ΔV_T relative to that for octahedral site ΔV_0.

$f(R)$	Parameter value	a_s/a_E [Eq. (36)]	$\Delta V_T/\Delta V_0$
$e^{-\alpha R}$	$\alpha R_0=3.4$	3.1	0.91
R^{-p}	$p=2.4$	3.3	0.94
$e^{\gamma/R}$	$\gamma/R_0=1.4$	3.4	0.95

$n_E=6$, $N_E=12$, and $n_s=N_s=3$ for an octahedron). If it can be assumed that $V(R)$ is sufficiently well behaved between R_0 and R_s that it can be approximated by a simple function, such as a power law, then a_s/a_E is determined. Table II gives the resulting values of a_s/a_E for the form $V(R)=V(R_0)+Af(R)$ with $f(R)=e^{-\alpha R}$, R^{-p}, and $e^{\gamma/R}$. Since only a ratio of derivatives is involved, the results depend only on α, p, and γ and are independent of the constants A and $V(R_0)$. These constants do influence the activation energy, and thus it seems likely that the parameter a_s needed for the width of the distribution of activation energies can be considerably less sensitive to details of the potential than is the activation energy itself. This is borne out by Table II where only a 10% variation in a_s is seen.

The above equations are based on the premise that the linear approximations of Appendix A and Eq. (16) hold. This requires $R_s V'(R_s)Y_\alpha/V(R_s)\ll 1$. At the root-mean-square value $\langle Y_\alpha^2\rangle^{1/2}=\sqrt{3/2}\sigma$, we find

$$R_s V'(R_s)\langle Y_\alpha^2\rangle^{1/2}/V(R_s)\approx 0.25$$

for $\sigma=0.07$ and the parameters given in Table II; so there is reasonable consistency. If, however, the potential is much more steeply varying at R_s (i.e., hard-core-like) than can be accounted for by any of the simple expressions of Table II, one has to be more careful. We show in Appendix A that for a hard-core-like potential combined with lattice relaxation, one might expect a_s/a_E to be reduced. It is obvious from Eq. (36) that $a_s/a_E=2\sqrt{2/3}=1.6$ represents a lower limit to the ratio, since the hydrogen-metal force at the saddle point is at least as great as at the equilibrium point.

It is also of interest to compare the volume expansion expected for hydrogen at a tetrahedral site with that for hydrogen at an octahedral site. Equations (3) and (5) show that

$$\Delta V_T/\Delta V_0=\frac{1}{\sqrt{3}}\frac{V'(R_T)}{V'(R_0)}, \tag{37}$$

where $R_T=\sqrt{3/8}d_0$ and ΔV_T are tetrahedral site parameters. The ratio is given in Table II, the noteworthy fact being that there is less than a 10% difference between ΔV_T and ΔV_0. Thus one cannot conclude from the volume change alone that hydrogen occupies octahedral sites in $Pd_{80}Si_{20}$. The mean activation energy and width predicted from Eqs. (26) and (27) are shown versus effective concentration in Figs. 3 and 4, respectively, for $a_s/a_E=3$ (soft potential value, Table II) and $a_s/a_E=1.6$ (lower limit). The complete distribution given by Eqs. (25) and (26) is shown in Fig. 5 for $a_s/a_E=1.6$ and $c=1\%$. Also shown are the data from Ref. 3 which are for hydrogen-metal concentrations of a few percent. (The "true" concentration N_H/N_A, where N_H and N_A are the number of hydrogen and host atoms, respectively, differs from the effective concentration used here, $c=N_H/N_S$ for N_S equilibrium sites. For octahedral sites, in a distribution of soft spheres, the work of Ref. 9 gives $N_S\approx N_A/4$, while $N_S\approx 2.5N_A$

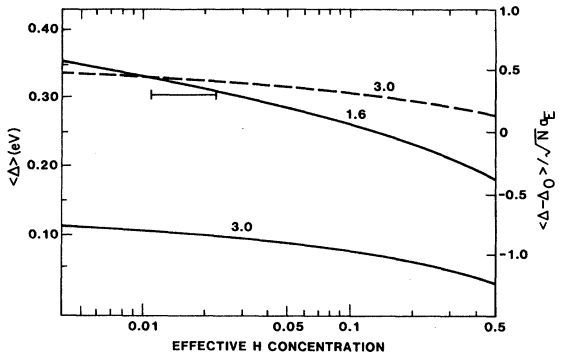

FIG. 3. Mean activation energy for H in $Pd_{80}Si_{20}$, using $\Delta_0=0.25$ eV, $a_E=0.8$ eV, $N=12$ (octahedral site). Solid curves are Eq. (26). Dashed curve is Eq. (26) with $\langle \delta Y_{\alpha\max}\rangle=0$, which corresponds to distribution for hopping out of one face. Numbers beside curves are values of a_s/a_E. Horizontal bar is value from distribution used to fit data in Ref. 3.

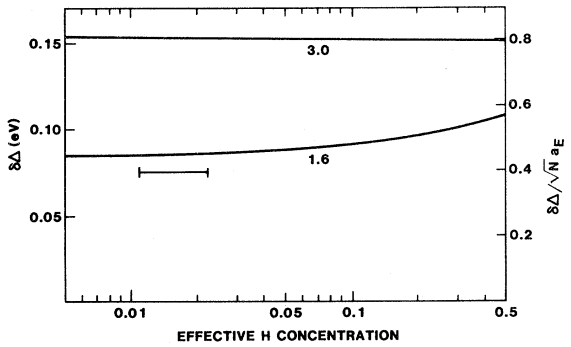

FIG. 4. Effective Gaussian width of distribution of activation energies for H in $Pd_{80}Si_{20}$, using $\Delta_0=0.25$ eV, $a_E=0.8$ eV, $N=12$ (octrahedral site). Curves are Eq. (27) for values of a_s/a_E shown. Horizontal bar is value from distribution used to fit data in Ref. 3.

if both octahedral and tetrahedral sites are included. Thus $N_H/N_A=0.01$ corresponds to $c\approx 0.04$ if only octahedral sites are counted.)

The width is somewhat broader than observed even for the smallest allowable a_s/a_E. The larger value of a_s/a_E gives much too large a contribution to the negative shift in Δ, which arises from the term proportional to $\langle \delta Y_{\alpha\max}\rangle$ in Eq. (25). The distribution for hopping through any one face α with activation energy $\Delta_{i\alpha}$ does not contain this negative shift and therefore gives a much larger activation energy which, as shown in Fig. 3, is in reasonable agreement for the larger a_s/a_E ratio. However, the width for this distribution is about 0.25 eV at $a_s/a_E=3$, which is much too large. Also, as discussed earlier, we rule it out on the grounds that experiments should measure the total rate for hopping through all faces. Validity of the low-temperature approximation requires

$$\exp[\beta a_s\langle \delta Y_{\alpha\max}\rangle]\gg 1$$

so that the largest exponential in the summation in Eq. (17) dominates. For the minimum $a_s/a_E\sim 1.6$, we have $\beta a_s\langle \delta Y_{\max}\rangle\sim 5$ at 250 K with $a_E=0.8$ eV, so that the condition is well satisfied. By comparison, the high-temperature approximation (18) gives widths of 0.048 and 0.11 eV for $a_s/a_E=3$ and $a_s/a_E=1.6$, respectively. Note the opposite dependence upon a_s/a_E for this range of values because the term in δY_α is absent.

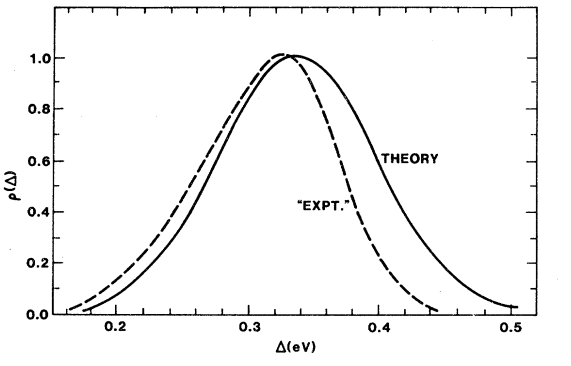

FIG. 5. Distribution of activation energies for H in $Pd_{80}Si_{20}$. "Theory" curve is result of using Eqs. (25) and (28)–(30) in (25) with $\Delta_0=0.25$ eV, $a_E=0.8$ eV, $a_s/a_E=1.6$, $c=1\%$. "Experiment" curve is distribution used to fit data in Ref. 3.

IV. DISCUSSION

The closest agreement with experiment is obtained by taking a_s/a_E to be its smallest physically allowable value rather than as given in Table II for model potentials. The values for a_s/a_E in Table II neglect lattice relaxation, since they assume that the hydrogen-metal force is the same as if the cage were rigid. Allowing the metal lattice to relax obviously reduces this force, i.e., it is less at the relaxed hydrogen-metal distance. Thus it may be reasonable to expect a smaller a_s/a_E. This point is discussed quantitatively in Appendix A.

The distribution of activation energies used to fit the data in Ref. 3 was asymmetric with the width on the low-energy side about twice that on the high-energy side. Our results do not reproduce this feature, as is evident by the nearly symmetric-curve in Fig. 5. However, although a best fit to the data is obtained with the asymmetric Gaussian, I find that nearly as good a fit results from a simple symmetric Gaussian, so this lack of agreement may not be too important.

One might be happier if agreement were obtained with a larger value of a_s/a_E than with the minimum acceptable one. This would require a distribution $\rho(Y_{\alpha\max}\mid Y)$ which is both narrower and less skewed toward large $\delta Y_{\alpha\max}$ than given by Eq. (25). Both of these would be accomplished by introducing some correlation between the probability for sides d_2 and d_3 of a triangle, given the first side d_1 rather than using Eq. (6), which neglects any such correlation. However, the fact that the uncorrelated distribution of Eq. (8) seems to reproduce the results found in Ref. 9 would argue against any strong correlation.

There is a distribution of hydrogen vibrational frequencies ω_0 as well as site energies. From Eq. (34) and the parameters for an exponential potential given in Table II, we estimate the width to be $\delta\hbar\omega_0=1.4$ meV for $\hbar\omega_0=66$ meV. This is considerably smaller than the site energy width of 190 meV,

which justifies its neglect in the present paper.

In the absence of thermal weighting so that $\langle Y \rangle = 0$, we predict a negative shift in activation energy since the net hopping rate is determined by the face with the lowest barrier rather than the average barrier of all the faces. An activation energy less than the crystalline value was also found in Ref. 9 for hopping out of octahedral sites. But the reason appears to be quite different. They assumed that the site energy for an octahedron was determined by the *shortest* of the three metal-metal distances passing through the center of an octahedron. Thus their distribution of octahedron sizes was peaked at $R < d/\sqrt{2}$ [see Fig. 13(b) of Ref. 9]; the mean site energy was correspondingly higher and hence the activation energy lower. Since their tetrahedron and triangle sizes are defined instead as an average distance from vertices,[19] the mean energy does not deviate appreciably from the crystalline value for these figures. As a result, they found a reduction in activation energy only for hopping out of an octahedron.

I would argue on the basis of Eq. (2) and Appendix A that the site energy is always the crystalline value if there is no weighting by thermal population factors. The activation energy is lowered because it is governed by the distribution of the *largest* triangle faces. That is, in my view, the appropriate saddle-point energy is lowered and the site energy unchanged from the crystalline value, whereas Ahmadzadeh and Cantor have unchanged saddle-point and increased octahedral site energy. The work here predicts a similar effect for jumping out of tetrahedral sites, in disagreement with Ref. 9.

Although the distribution of activation energies derived here appears to fit the internal-friction data fairly well, there is one disturbing feature which must be mentioned. The strength of the internal-friction peak is much more suggestive of a very anisotropic site geometry, such as the hydrogen sitting at the center of a dumbbell, than of the symmetric tetrahedral or octahedral environment. The existence of hydrogen-related internal friction requires that the hydrogen hop between sites whose energy difference changes with applied uniaxial stress. Thus there is no internal friction for octahedral sites in the ideal fcc structure since these sites of cubic symmetry are all equivalent, even under uniaxial stress. The octahedral sites in an amorphous system can show internal friction because (i) the octahedra can be distorted from cubic symmetry and (ii) there is a stress-dependent change in energy as a function of size of the octahedron so that even regular octahedra of varying sizes can contribute. However, it is difficult to see how these effects can produce an internal friction peak as big as for highly anisotropic sites, which seems to be required.

Bulk diffusion, which requires many hops, has not been treated here. Our distribution of activation energies strictly holds only for situations in which relaxation or decorrelation is effectively achieved in one hop from an equilibrium configuration, as is expected to be the case for microscopic phenomena such as NMR or internal friction. We have avoided questions related to the path a particle takes once it leaves the equilibrium site. These would have to be addressed in discussing bulk migration such as is observed in the Gorsky effect.

V. SUMMARY AND CONCLUSIONS

The distribution of activation energies has been derived for a small impurity such as hydrogen hopping in an amorphous metal. Classical over-the-barrier motion was assumed so that the activation energy is the difference between saddle-point and equilibrium-site energies. The equilibrium sites were taken as centers of octahedra for specific applications, although formulas were derived for general polyhedra. The saddle point was the center of a triangular face of the polyhedron. The dimensions of the triangles and polyhedra vary in a manner which was predicted from the radial distribution function (RDF). The results agreed well with the interstitial-size distributions reported in Ref. 9.

The site energy distribution was related to the RDF and to observed hydrogen-induced volume change without having to know details of the hydrogen-metal potential, similar to what was done in Ref. 6. The saddle-point distribution is more subtle in two aspects. First, we showed that, for the relatively low temperatures of interest, the particle hops through the face with the lowest saddle-point energy, i.e., the triangle which has the largest size. This led to consideration of the conditional probability for the size of the largest face of an octahedron given the sum of all the edge lengths of the octahedron. Second, the proportionality between size and energy at the saddle point must be estimated from a model potential. This was done by fitting the known volume expansion and hydrogen vibrational frequency at the equilibrium point in the crystalline material to simple functional forms of the potential and also by considering a hard-core potential at the saddle point together with lattice relaxation.

Results were compared with the distribution of activation energies required to fit the internal-friction data for H in $Pd_{80}Si_{20}$, and good agreement was found. The only adjustable parameter in the theory is a_s/a_E, which is proportional to the ratio of hydrogen-metal force at the saddle point and to that

at the equilibrium point. Based on the known volume expansion and hydrogen vibrational frequency together with physical reasoning for lattice relaxation, we estimated that $1.6 < a_s/a_E \lesssim 3$. The data are best fitted for a_s/a_E at the lower limit.

Since most amorphous metal alloys seem to have similar RDF's and local potentials which are the same as in the crystal, the methods used here should be applicable to hydrogen or other small interstitials in a variety of amorphous materials. A distribution of activation energies has commonly been invoked to explain relaxation data; but in the past it has generally been chosen only to give agreement without any first-principles considerations. The present study shows that such distributions can be placed on much firmer foundations.

ACKNOWLEDGMENTS

This work was performed at Sandia National Laboratories and was supported by the U. S. Department of Energy under Contract No. DE-AC04-76DP000789.

APPENDIX A: EQUILIBRIUM ENERGY OF PARTICLES IN A DISTORTED POLYHEDRON

As in the main text, the n vertices of the distorted polyhedron are at positions $\vec{R}_i = \vec{R}_i^0 + \vec{r}_i$, $i = 1,2, \ldots, n$, where $|\vec{R}_i^0| = R_0$ and $\sum_i^n \vec{R}_i^0 = 0$. The equilibrium position is $\vec{r} = 0$ for the regular figure with $\vec{r}_i = 0$; so for small distortions the energy at the new equilibrium position $\vec{r}$ is

$$U(\vec{r}) = \sum_{i=1}^{n} V(\vec{R}_i) + O(r^2) , \tag{A1}$$

since the term linear in r must vanish if $\vec{r}$ is the equilibrium position. It therefore follows that to first order in r_i

$$U(\vec{r}) = nV(R_0) + \frac{V'(R_0)}{R_0} \sum_{i=1}^{n} \vec{r}_i \cdot \vec{R}_i^0 . \tag{A2}$$

The vector between vertices i and j is $\vec{d}_{ij} = \vec{R}_i - \vec{R}_j$ so that to lowest order the edge length is

$$d_{ij} = d_0 + (\vec{r}_i - \vec{r}_j) \cdot (\vec{R}_i^0 - \vec{R}_j^0)/d_0 , \tag{A3}$$

where d_0 is the edge length of the undistorted figure and i and j are meant to be nearest-neighbor vertices.

Consider the sum over all edge lengths d_{ij}. This will be proportional to $\sum_{i=1}^{n} \vec{r}_i \cdot \vec{R}_i^0$, provided that $\sum_{j(i)} \vec{R}_j^0(i)$ either is zero or is proportional to $\vec{R}_i^0$ so that the cross terms from Eq. (A3) vanish. Here $j(i)$ is a vertex which is a distance d_0 from vertex i. The former is true for the octahedron since, for example, with $\vec{R}_i^0 = R_0(0,0,1)$, the vectors $\vec{R}_{j(i)}^0$ are $R_0(\pm 1,0,0)$ and $R_0(0,\pm 1,0)$. For the triangle or tetrahedron every vertex $j \neq i$ is a distance d_0 from vertex i, so that $\sum_{j(i)} \vec{R}_j^0 + \vec{R}_i^0 = \sum_i \vec{R}_i^0 = 0$, whereby the latter condition is met. Hence at least for the figures of interest here it follows that

$$\sum_{i=1}^{n} \vec{r}_i \cdot \vec{R}_i^0 / R_0 = C \sum_{k=1}^{n} (d_k - d_0) , \tag{A4}$$

where C is a constant and d_{ij}, the distance between neighboring vertices i and j, has been relabeled as d_k for the kth edge. C is readily determined by noting that for the special case where $\vec{r}_i$ is of constant magnitude δ in the direction of $\vec{R}_i^0$ one must have a constant $d_k = d_0 + \delta(d_0/R_0)$. Thus

$$C = \frac{n}{N} \left[\frac{R_0}{d_0} \right] , \tag{A5}$$

so that (A2) becomes

$$U(r) = nV(R_0) + \frac{n}{N} R_0 V'(R_0) \sum_{k=1}^{N} (d_k - d_0)/d_0 , \tag{A6}$$

which is the same as Eq. (2).

Displacement of the metal atoms by lattice relaxation has thus far been neglected. If introduction of hydrogen causes a displacement $\vec{\epsilon}_i$ of the metal atom from its position $\vec{R}_i^0 + \vec{r}_i$ in the distorted figure, then Eq. (A1) is modified to

$$U = \sum_{i=1}^{n} V(\vec{R}_i + \vec{\epsilon}_i) + \tfrac{1}{2} \sum_{i=1}^{n} \sum_{j=1}^{n} \sum_{\alpha\beta} k_{ij}^{\alpha\beta} \epsilon_i^{\alpha} \epsilon_j^{\beta} \tag{A7}$$

for the total energy where the second term represents elastic energy of the metallic host. The quantity $k_{ij}^{\alpha\beta}$ is an effective force tensor which can include effects of distant strains, and it has been assumed that $\vec{\epsilon}_i = 0$ corresponds to equilibrium of the metal host.

If, as may be the case at the saddle point, the potential is rapidly varying, an expansion such as (A2) about $\vec{\epsilon}_i = 0$ is not legitimate. However, we assume that an expansion is allowed at the relaxed position, so that Eq. (A7) can be written as

$$U \approx \sum_{i=1}^{n} V(R_0 + \epsilon) + \frac{V'(R_0 + \epsilon)}{R_0} \sum_{i=1}^{n} \vec{r}_i \cdot \vec{R}_i^0 + \frac{n k_0 \epsilon^2}{2} , \tag{A8}$$

as long as $V'(R_0 + \epsilon + r_i)$ is well behaved for small

r_i, even though $V'(R_0+r_i)$ may not be. In arriving at (A8), symmetry has been assumed whereby $\vec{\epsilon}_i=\epsilon\vec{R}_i^0/R_0$ and $k_{ij}^{\alpha\beta}=k_{ij}\delta_{\alpha\beta}$ with $k_0=\sum_j k_{ij}$, and $\epsilon \ll R_0$ has also been used. As long as

$$r_i V'(R_0+\epsilon) \ll V(R_0+\epsilon) ,$$

the second term on the right-hand side, involving r_i, does not affect the value of ϵ obtained by minimizing U. Thus apart from a shifted energy at $r_i=0$ which does not affect the width of the distribution, Eq. (A6) may be used with the force $V'(R_0)$ evaluated at the relaxed distance $R_0+\epsilon$ where it is assumed to be moderate. As a result the ratio between forces at the saddle-point and equilibrium positions can be considerably less than estimated in the absence of relaxation. The extreme limit occurs when ϵ is sufficiently large to make the relaxed hydrogen-metal distance the same at the saddle-point and equilibrium positions.

APPENDIX B: CONDITIONAL PROBABILITIES

We consider here the conditional probabilities $\rho(Y_1,Y_2,\ldots,Y_F \mid Y)$ and $\rho(Y_{\alpha\max} \mid Y)$ for a polyhedron with F faces where

TABLE III. Moments of conditional probabilities $\rho(X \mid Y)$.

X	$\langle X\rangle$	$\langle (X-\langle X\rangle)^2\rangle$
Y_α	$2Y/F$	$3k\sigma^2/2$
$Y_{\alpha\max}$	$2Y/F+\sqrt{3}k\sigma(1.01)$[a]	$3k\sigma^2(0.19)$[a]

[a]Numerical result from Eq. (B20) with $F=8$. $k=1-2/F$; other quantities are defined in the first paragraph of Appendix B.

$$Y=\sum_{i=1}^{N}\left[\frac{d_i}{d_0}-1\right]\equiv\sum_{i=1}^{N} y_i \tag{B1}$$

is the deviation of the sum of the N edges from the ideal value Nd_0 normalized to the regular edge length d_0; $Y_\alpha=y_{\alpha1}+y_{\alpha2}+y_{\alpha3}$ is the deviation for the sum of the edges of the face α, the faces assumed to be triangles, and $Y_{\alpha\max}$ is the largest of the F values of Y_α. The final results are summarized in Table III. The edge deviations y_i are assumed to be independent so that their distribution is

$$\rho_N(y_1,y_2,\ldots,y_N)=\rho(y_1)\rho(y_2)\cdots\rho(y_N) , \tag{B2}$$

where $\rho(y_i)$ is the RDF. The unrestricted distribution for a single face is

$$\rho(Y_\alpha)=\int dy_1\int dy_2\int dy_3\rho(y_1)\rho(y_2)\rho(y_3)\delta(y_1+y_2+y_3-Y_\alpha)=\int_{-\infty}^{\infty} dt\, e^{-iY_\alpha t}[\tilde{\rho}(t)]^3 , \tag{B3}$$

where $\tilde{\rho}(t)=\int_{-\infty}^{\infty} dy\,\rho(y)e^{iyt}$ and we have used the identity $\delta(x)=(1/2\pi)\int_{-\infty}^{\infty} e^{ixt}dt$. For a Gaussian RDF this reduces to

$$\rho(Y_\alpha)=e^{-Y_\alpha^2/3\sigma^2} , \tag{B4}$$

where, as in the main text, we ignore any multiplicative constants, either which result in the course of performing integrations or which are required for normalization. Similarly, the unrestricted distribution for the F faces is

$$\begin{aligned}\rho(Y_1,Y_2,\ldots,Y_F)&=\int dy_1\rho(y_1)\cdots\int dy_N\rho(y_N)\delta(y_1+y_2+y_3-Y_1)\\&\quad\times\delta(y_1+y_4+y_5-Y_2)\cdots\delta(y_{N-2}+y_{N-1}+y_N-Y_F)\\&=\int_{-\infty}^{\infty} dt_1 e^{-iY_1t_1}\cdots\int_{-\infty}^{\infty} dt_F e^{-iY_Ft_F}\tilde{\rho}(t_1+t_2)\cdots\tilde{\rho}(t_i+t_j)\cdots ,\end{aligned} \tag{B5}$$

where the edges and faces are numbered so that face 1 has edges 1, 2, and 3, face 2 has edges 1, 4, and 5, and so on. Each edge is common to two triangles so that if $\tilde{\rho}(t_i+t_j)$ in the expression is the transform of $\rho(y_k)$, then t_i and t_j represent the two faces which are common to edge k. Since each triangular face shares edges with three other faces, the integrals in (B5) are not easily separable in general. For a Gaussian $\rho(y)$, and therefore for $\tilde{\rho}(t)$ also, the product of $\tilde{\rho}$'s in (B5) becomes

$$\begin{aligned}\tilde{\rho}(t_1+t_2)\cdots\tilde{\rho}(t_i+t_j)&=\exp\left[\frac{\sigma^2}{4}[(t_1+t_2)^2+\cdots+(t_1+t_j)^2+\cdots]\right]\\&=\exp\left[\frac{\sigma^2}{4}(3t_1^2+3t_2^2+\cdots+3t_N^2+2t_1t_2+\cdots+2t_it_j+\cdots)\right] ,\end{aligned} \tag{B6}$$

where the factor of 3 in $3t_i^2$ comes from the fact that each face has three edges and thus must be represented three times in the sum over edges. The cross terms prevent the left-hand side of (B5) from being a simple product of Gaussians. A nice simplification, however, occurs for a tetrahedron where each face is in contact with all the other faces. Then it is evident by symmetry that the sum over t's must be expressible as

$$3t_1^2+3t_2^2+\cdots+3t_N^2+2t_1t_2+2t_it_j+\cdots=a\left[\sum_{i=1}^{N}t_i^2\right]+bT^2 \quad (N=6,\ \text{tetrahedron}), \tag{B7}$$

where $T=\sum_{i=1}^{N}t_i$ and a and b are appropriate constants. It is also easy to see that $a=2$, $b=1$. In this case (B5) becomes

$$\rho(Y_1,Y_2,Y_3,Y_4)=\int_{-\infty}^{\infty}dz\,e^{-izT}e^{-\sigma^2T^2/4}\prod_{\alpha=1}^{4}\int_{-\infty}^{\infty}dt\exp[-\sigma^2(2t^2)/4]\exp[-i(Y_\alpha-z)t], \tag{B8}$$

which gives

$$\rho(Y_1,Y_2,Y_3,Y_4)=\exp\left[-\frac{1}{2\sigma^2}\left[\sum_{\alpha=1}^{4}Y_\alpha^2-\tfrac{2}{3}Y^2\right]\right]. \tag{B9}$$

The term in Y^2 acts like a constant for the conditional probability so that an exact expression for the unnormalized conditional probability for the tetrahedron is

$$\rho(Y_1,Y_2,Y_3,Y_4\mid Y)=\exp\left[-\frac{1}{2\sigma^2}\left[\sum_{\alpha=1}^{4}Y_\alpha^2\right]\right]\delta(Y_1+Y_2+Y_3+Y_4-2Y). \tag{B10}$$

Note that since each edge is common to two triangles, it follows that

$$\sum_{\alpha=1}^{F}Y_\alpha=2\sum_{i=1}^{N}y_i=2Y,$$

and $3F=2N$.

In the language of statistical mechanics, the δ function in Eq. (B10) represents a microcanonical ensemble. For large numbers of "particles" (faces, in this case), one goes to grand-canonical ensemble in which

$$\delta\left[\sum_{\alpha=1}^{F}Y_\alpha-2Y\right]$$

is replaced by

$$\exp\left[-\lambda\sum_{\alpha=1}^{F}Y_\alpha\right],$$

where the multiplier λ is chosen to give the correct average $\langle Y_\alpha\rangle=2Y/F$. The δ function has no significant effect on the fluctuation $\langle Y_\alpha^2\rangle-\langle Y_\alpha\rangle^2$ for large numbers of particles; one keeps the same value of σ in the grand-canonical ensemble when dealing with statistical mechanics of 10^{23} particles. Here the situation is different because $F=4$ (tetrahedron) or 8 (octahedron) is not astronomically large. We therefore make the ansatz

$$\rho(Y_1,\ldots,Y_2,\ldots,Y_F\mid Y)=\prod_{\alpha=1}^{F}\exp(-\delta Y_\alpha^2/3k\sigma^2), \tag{B11}$$

where $\delta Y_\alpha=Y_\alpha-2Y/F$, and k is a constant introduced to give the same fluctuation

$$\langle(\delta Y_\alpha)^2\rangle_Y=\tfrac{3}{2}k\sigma^2 \tag{B12}$$

as in the microcanonical distribution such as (B10). (The subscript Y indicates that the average is taken with respect to a conditional distribution.) It is obvious that $\langle\delta Y_\alpha\rangle=0$ for (B11) so that the implied choice of the multiplier

$$\lambda=2\langle Y_\alpha\rangle/3k\sigma^2=4Y/3k\sigma^2F$$

is justified (a constant term $\langle Y_\alpha\rangle^2/3k\sigma^2$ has also been added in the exponent). The quantity k differs from unity not only because of the δ function, but also because the faces share edges. It is determined by noting that

$$\langle(\delta Y_\alpha)^2\rangle_Y=\langle(y_1+y_2+y_3)^2\rangle_Y-4Y^2/F^2, \tag{B13}$$

where $y_1+y_2+y_3$ is the perimeter deviation for the face α and using, from Eq. (B2) with a δ function added for the conditional distribution,

$$\langle(y_1+y_2+y_3)^2\rangle_Y=\frac{\int\cdots\int dy_1\cdots dy_N\exp\left[\frac{-1}{\sigma^2}\sum_{i=1}^{N}y_i^2\right](y_1+y_2+y_3)^2\delta\left[\sum_{i=1}^{N}y_i-y\right]}{\int\cdots\int dy_1\cdots dy_N\exp\left[\frac{-1}{\sigma^2}\sum_{j=1}^{N}y_j^2\right]\delta\left[\sum_{j=1}^{N}y_j-Y\right]}. \tag{B14}$$

The numerator is

$$3\int_{-\infty}^{\infty} dt\, e^{-iYt}\left[\int_{-\infty}^{\infty} y_1^2 e^{-y_1^2/\sigma^2} e^{iy_1 t} dy_1 \left[\int_{-\infty}^{\infty} e^{-y^2/\sigma^2} e^{iyt} dy\right]^{N-1}\right.$$
$$\left.+2\left[\int_{-\infty}^{\infty} y_1 e^{-y_1^2/\sigma^2} e^{iy_1 t} dy_1\right]^2 \left[\int_{-\infty}^{\infty} e^{-y^2/\sigma^2} e^{iyt} dy\right]^{N-2}\right]$$
$$=3(\pi\sigma^2)^{N/2}\sigma^2\int_{-\infty}^{\infty} dt\, e^{-iYt}\exp(-N\sigma^2 t^2/4)(\tfrac{1}{2}-3\sigma^2 t^2/4)\,, \quad \text{(B15)}$$

while the denominator is

$$\int_{-\infty}^{\infty} dt\, e^{-iYt}\left[\int_{-\infty}^{\infty} e^{-y^2/\sigma^2} e^{iyt} dy\right]^N = (\pi\sigma^2)^{N/2}\int_{-\infty}^{\infty} dt\, e^{-iYt}\exp(-N\sigma^2 t^2/4)\,, \quad \text{(B16)}$$

so that the ratio is

$$\langle (y_1+y_2+y_3)^2\rangle_Y = \frac{3\sigma^2}{2}\left[1-\frac{3\int_{-\infty}^{\infty} dt\,\sigma^2 t^2 e^{-iYt}\exp(-N\sigma^2 t^2/4)}{2\int_{-\infty}^{\infty} dt\, e^{-iYt}\exp(-N\sigma^2 t^2/4)}\right]$$
$$=(\tfrac{3}{2})\sigma^2[1-3/N]+9Y^2/N^2=(\tfrac{3}{2})\sigma^2[1-2/F]+4Y^2/F^2\,, \quad \text{(B17)}$$

and thus, by comparing with (B12)

$$k=1-2/F\,. \quad \text{(B18)}$$

The conditional probability $\rho(Y_\alpha \mid Y)$ for a single face evidently is just

$$\rho(Y_\alpha \mid Y)=\exp[-(\delta Y_\alpha)^2/3k\sigma^2]\,, \quad \text{(B19)}$$

since according to (B11) the faces have been made independent by introduction of the grand ensemble. For $\rho(Y_{\alpha\max} \mid Y)$ we integrate over the other faces $\alpha\neq\alpha\max$ subject to the condition that $Y_\alpha < Y_{\alpha\max}$. Thus

$$\rho(Y_{\alpha\max} \mid Y)=\exp[-(\delta Y_{\alpha\max})^2/3k\sigma^2]\left[\int_{-\infty}^{\delta Y_{\alpha\max}} d\delta\, Y_\alpha \exp[-(\delta Y_\alpha)^2/3k\sigma^2]\right]^{F-1}$$
$$=\exp[-(\delta Y_{\alpha\max})^2/3k\sigma^2][\operatorname{erfc}(-\delta Y_{\alpha\max}/\sqrt{3k}\,\sigma)]^{F-1}\,. \quad \text{(B20)}$$

Since the distribution in Eq. (B20) is a function only of $\delta Y_{\alpha\max}$, it follows that Y and $\delta Y_{\alpha\max}$ are statistically independent, $\langle Y\delta Y_{\alpha\max}\rangle=\langle Y\rangle\langle\delta Y_{\alpha\max}\rangle$. The moments of (B20) for $F=8$ are shown in Table III.

It should be noted that in going from Eq. (B5) to (B11) for a tetrahedron, the only approximation has been the use of the grand ensemble with properly adjusted width for a small number of "particles." This is because of the validity of Eq. (B7) for a tetrahedron. Unfortunately, it is not valid for the octahedron. Since there are eight faces, and each face shares an edge with only three others, evidently there are several cross terms $t_i t_j$ in T^2 which do not appear in (B6). For simplicity, however, we have assumed that the form (B11) can be used for any polyhedron with k chosen to give the correct mean-square width of the distribution.

[1]See G. S. Cargill, III, in *Solid State Physics,* edited by H. Ehrenreich, F. Seitz, and D. Turnbull (Academic, New York, 1975), Vol. 30, p. 227.

[2]Y. Takagi and K. Kawamura, Trans. Jpn. Inst. Met. 22, 677 (1981).

[3]B. S. Berry and W. C. Pritchet, Phys. Rev. B 24, 2299 (1981).

[4]A. S. Nowick and B. S. Berry, *Anelastic Relaxation in Crystalline Solids* (Academic, New York, 1972).

[5]K. L. Ngai, Solid State Ionics 5, 27 (1981); A. K. Jonscher, Nature 267, 673 (1977).

[6]R. Kirchheim, F. Sommer, and G. Schlückebier, Acta.

Metall. 30, 1059 (1982).
[7]K. W. Kehr, in *Hydrogen in Metals I,* edited by G. Alefeld and J. Völkl (Springer, New York, 1978), Chap. 8; J. Volkl and G. Alefeld, *ibid.*, Chap. 12.
[8]J. L. Finney and J. Wallace, J. Non-Cryst. Solids 43, 165 (1981).
[9]M. Ahmadzadeh and B. Cantor, J. Non-Cryst. Solids 43, 189 (1981).
[10]H. Wagner, in text of Ref. 7, Chap. 1.
[11]J. R. Hardy, J. Phys. Chem. Solids 29, 2009 (1968).
[12]D. E. Polk, Acta. Metall. 485 (1972); D. S. Boudreaux and H. J. Frost, Phys. Rev. B 23, 1506 (1981).
[13]J. E. Worsham, Jr., M. K. Wilkinson, and C. G. Shull, J. Phys. Chem. Solids 3, 303 (1957).
[14]H. Peisl, in text of Ref. 7, Chap. 3.
[15]K. A. Gschneidner, in *Solid State Physics,* edited by H. Ehrenreich, F. Seitz, and D. Turnbull (Academic, New York, 1964), Vol. 16, p. 275.
[16]Y. Waseda and T. Egami, J. Mater. Sci. 14, 1249 (1979); J. F. Graczyk, Phys. Status Solidi 60, 323 (1980).
[17]L. V. Heimendahl, J. Phys. F 5, L141 (1975).
[18]T. S. Springer, in text of Ref. 7, Chap. 4.
[19]I am grateful to Dr. B. Cantor for a private communication on this point.